

# Isogeometric Analysis of Finite Deformation Solids

Kjell Magne Mathisen<sup>†</sup>, Knut Morten Okstad<sup>‡</sup> and Trond  
Kvamsdal<sup>‡</sup>

<sup>†</sup>NTNU, Department of Structural Engineering, Trondheim, Norway

<sup>‡</sup>SINTEF ICT, Department of Applied Mathematics, Trondheim, Norway

January 26, 2012

# Outline

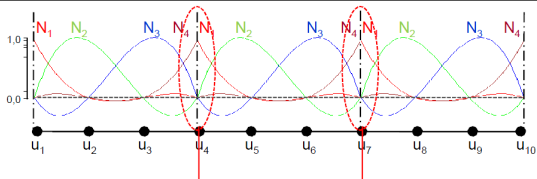
- ▶ Motivation
- ▶ NURBS vs. Lagrange FEM
- ▶ Nonlinear elasticity
- ▶ Mixed formulation
- ▶ Implementational issues
- ▶ Numerical examples
- ▶ Concluding remarks

# Motivation

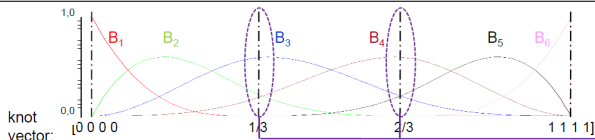
- ▶ "Locking" – a challenge in linear as well as nonlinear problems
- ▶ Volumetric locking – a challenge where nearly incompressible behavior is prevalent
- ▶ NFEA has been dominated by use of low-order elements designed to avoid volumetric or incompressible locking
- ▶ Recently the isogeometric approach has formed the basis for overcoming the incompressibility problem
  - ▶ Hughes and co-workers has addressed this by the  $\bar{B}$  and  $\bar{F}$ -projection methods
  - ▶ Taylor improved the performance of mixed elements by using NURBS
- ▶ We have implemented two classes of mixed elements into *IFEM*, an object-oriented toolbox for performing isogeometric NFEA with splines and NURBS as basis functions

# B-splines vs Lagrange shape functions in 1D

$C^0$  – continuity  $\Rightarrow$  discontinuous stress/strain fields between elements



$C^{p-1}$  – continuity  $\Rightarrow$  continuous stress/strain fields for  $p \geq 2$



NURBS can exactly represent conical sections

**Note:** Number of control points less than number of nodal points  $\Rightarrow$  B-Splines obtain higher accuracy vs dofs invested for Lagrange

# Comparison of FEA and IGA:

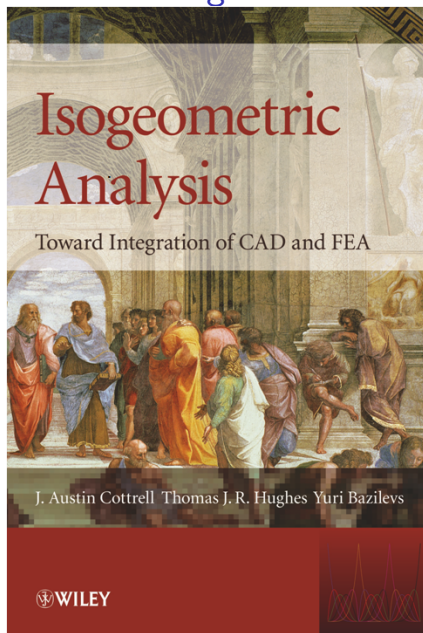
## Finite Element Analysis:

- ▶ Nodal points
- ▶ Nodal variables
- ▶ Mesh
- ▶ Lagrange basis functions
- ▶ Basis interpolate nodal points and variables
- ▶  $h$ -refinement
- ▶  $p$ -refinement
- ▶ Approximate geometry
- ▶ Subdomains

## Isogeometric Analysis:

- ▶ Control points
  - ▶ Control variables
  - ▶ Knots
  - ▶ NURBS basis functions
  - ▶ Basis **does not** interpolate control points and variables
  - ▶ Knot insertion
  - ▶ Order elevation
  - ▶ Exact geometry
  - ▶ Patches
- ▶ Partition of unity
  - ▶ Isoparametric concept
  - ▶ Patch test satisfied

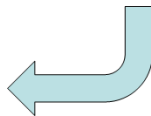
# Textbook on Isogeometric Analysis



## ICES

Institute for Computational  
Engineering and Sciences

Austin, Texas, U.S.A.



The authors, which are the originators of IGA, provide us with a systematic and comprehensive coverage on how to add isogeometric capabilities to FE programs

# Constitutive equations for finite hyperelasticity

# Hyperelasticity

- ▶ We assume hyperelastic homogeneous isotropic material behavior for which there exist a free-energy function<sup>1</sup>  $\Psi$  that depends on the left Cauchy-Green deformation tensor<sup>2</sup>  $\mathbf{b}$

$$\Psi = \Psi(\mathbf{b}) \quad \text{with} \quad \mathbf{b} = \mathbf{F}\mathbf{F}^T \quad \text{and} \quad \mathbf{F} = \mathbf{I} + \frac{\partial \mathbf{u}}{\partial \mathbf{X}}$$

$\mathbf{F}$  is the deformation gradient,  $\mathbf{u}$  is the displacement and  $\mathbf{I}$  is the 2nd order unit tensor

- ▶ Cauchy stresses  $\boldsymbol{\sigma}$  may be derived from the invariants of  $\mathbf{b}$

$$\boldsymbol{\sigma} = \frac{2}{J} \frac{\partial \Psi}{\partial \mathbf{b}} = \frac{2}{J} (\Psi_I \mathbf{b} + 2\Psi_{II} \mathbf{b}^2 + J^2 \Psi_{III} \mathbf{I})$$

$\Psi_I$ ,  $\Psi_{II}$  and  $\Psi_{III}$  are the derivatives of  $\Psi$  with respect to the invariants of  $\mathbf{b}$  and  $J = \det \mathbf{F}$ ; the determinant of the deformation gradient

---

<sup>1</sup>Also called stored energy or strain energy function

<sup>2</sup>Also referred to as the *finger* tensor

## Compressible neo-Hookean material model

- ▶ For hyperelastic materials exhibiting a completely different volumetric and isochoric response, the free-energy function may be additively decomposed into a volume-changing (dilatational part), and a volume-preserving (isochoric part)

$$\Psi(J, \mathbf{b}) = \Psi^{\text{dil}}(J) + \Psi^{\text{iso}}(J, \mathbf{b})$$

- ▶ The dilatational part is expressed in terms of  $J$

$$\Psi^{\text{dil}}(J) = \lambda U(J) = \frac{1}{2} \lambda (\ln J)^2$$

- ▶ The isochoric part is expressed in terms of  $J$  and  $\mathbf{b}$

$$\Psi^{\text{iso}}(J, \mathbf{b}) = \frac{1}{2} \mu (\text{tr} \mathbf{b} - 3) - \mu \ln J$$

- ▶  $\lambda$  and  $\mu$  are the Lamé's constants that may be derived from Young's modulus,  $E$ , and Poisson's ratio,  $\nu$

## Compressible neo-Hookean material model

- ▶ Cauchy stresses are obtained from the first derivatives of  $\Psi^{\text{dil}}$  and  $\Psi^{\text{iso}}$  w.r.t.  $J$  and the first invariant of  $\mathbf{b}$ ;  $I = \text{tr}\mathbf{b} = b_{kk}$

$$\begin{aligned}\sigma_{ij} &= \sigma_{ij}^{\text{dil}} + \sigma_{ij}^{\text{iso}} = \left( \lambda \frac{\partial U}{\partial J} + \frac{\partial \Psi^{\text{iso}}}{\partial J} \right) \delta_{ij} + \frac{2}{J} b_{ij} \frac{\partial \Psi^{\text{iso}}}{\partial I} \\ &= \frac{1}{J} [\mu b_{ij} + (\lambda \ln J - \mu) \delta_{ij}]\end{aligned}$$

- ▶ Spatial tangent moduli are similarly obtained from the second derivatives

$$c_{ijkl} = c_{ijkl}^{\text{dil}} + c_{ijkl}^{\text{iso}} = \frac{1}{J} [\lambda \delta_{ij} \delta_{kl} + 2(\mu - \lambda \ln J) \mathcal{I}_{ijkl}]$$

$$\text{where } \mathcal{I}_{ijkl} = \frac{1}{2} [\delta_{ik} \delta_{jl} + \delta_{il} \delta_{jk}]$$

## Modified neo-Hookean material model

- ▶ Rubber-like materials are characterized by relatively low shear modulus and high bulk modulus  $\Rightarrow$  they are nearly incompressible while highly deformable when sheared
- ▶ Multiplicative split of the deformation gradient into a volume-changing (dilatational) and volume-preserving (isochoric) part

$$\mathbf{F} = \mathbf{F}^{\text{dil}} \mathbf{F}^{\text{iso}} \quad \begin{cases} \mathbf{F}^{\text{dil}} = J^{1/3} \mathbf{I} & \Rightarrow \det \mathbf{F}^{\text{dil}} = \det \mathbf{F} = J \\ \mathbf{F}^{\text{iso}} = J^{-1/3} \mathbf{F} & \Rightarrow \det \mathbf{F}^{\text{iso}} = 1 \end{cases}$$

- ▶ A modified deformation gradient  $\bar{\mathbf{F}}$  is obtained by replacing  $J$  with the scalar parameter  $\bar{J}$  in the dilatational part

$$\bar{\mathbf{F}} = \bar{\mathbf{F}}^{\text{dil}} \mathbf{F}^{\text{iso}} = \left( \frac{\bar{J}}{J} \right)^{1/3} \mathbf{F} \quad \text{where} \quad \bar{\mathbf{F}}^{\text{dil}} = \bar{J}^{1/3} \mathbf{I} \Rightarrow \det \bar{\mathbf{F}} = \bar{J}$$

## Modified neo-Hookean material model

- ▶ Using the multiplicative split the isochoric part of the finger tensor becomes

$$\bar{\mathbf{b}} = \mathbf{b}^{\text{iso}} = \mathbf{F}^{\text{iso}}(\mathbf{F}^{\text{iso}})^T = J^{-2/3}\mathbf{b}$$

- ▶ The isochoric part of the free-energy function may now be written in terms of the modified invariant  $\bar{I} = \text{tr}\bar{\mathbf{b}} = J^{-2/3}\text{tr}\mathbf{b}$

$$\Psi(J, \bar{I}) = \Psi^{\text{dil}}(J) + \Psi^{\text{iso}}(\bar{I})$$

where

$$\Psi^{\text{dil}}(J) = \kappa U(J) = \frac{1}{4}\kappa (J^2 - 1 - 2 \ln J)$$

$$\Psi^{\text{iso}}(\bar{I}) = \frac{1}{2}\mu (\bar{I} - 3)$$

- ▶  $\kappa$  and  $\mu$  are equivalent to the small strain bulk and shear modulus, respectively

## Modified neo-Hookean material model

- ▶ The volumetric part of the Cauchy stresses for the above volumetric behavior gives rise to the hydrostatic pressure

$$\sigma_{ij}^{\text{dil}} = \kappa \frac{\partial U}{\partial J} \delta_{ij} = \frac{\kappa}{2J} (J^2 - 1) \delta_{ij}$$

- ▶ The deviatoric part now may be expressed in terms of the modified deformation tensor  $\bar{b}_{ij}$

$$\sigma_{ij}^{\text{iso}} = \frac{\mu}{J} \bar{b}_{ij}^{\text{d}} \quad \text{where} \quad \bar{b}_{ij}^{\text{d}} = \bar{b}_{ij} - \frac{1}{3} \delta_{ij} \bar{b}_{kk}$$

- ▶ Current spatial tangent moduli for the modified neo-Hookean material model

$$c_{ijkl} = c_{ijkl}^{\text{dil}} + c_{ijkl}^{\text{iso}}$$

where

$$c_{ijkl}^{\text{dil}} = \frac{\kappa}{J} \left[ J^2 \delta_{ij} \delta_{kl} + (1 - J^2) \mathcal{I}_{ijkl} \right]$$

$$c_{ijkl}^{\text{iso}} = \frac{2\mu}{3J} \left[ \bar{b}_{mm} (\mathcal{I}_{ijkl} - \frac{1}{3} \delta_{ij} \delta_{kl}) - \delta_{ij} \bar{b}_{kl}^{\text{d}} - \bar{b}_{ij}^{\text{d}} \delta_{kl} \right]$$

# Variational and discrete formulation of the finite deformation problem

## Mixed formulation

- ▶ A three-field mixed approximation has led to successful lower-order solid elements that can be used in finite deformation problems that exhibit compressible and/or nearly incompressible behavior for a large class of materials

$$\Pi(\mathbf{u}, p, \theta) = \int_{\Omega} \Psi(J, \bar{\mathbf{b}}) d\Omega + \int_{\Omega} p(J - \bar{J}) d\Omega - \Pi_{\text{ext}}$$

- ▶  $p$  is a Lagrange multiplier that constrains  $J$  to its independent representation, denoted  $\bar{J}$ .  $p$  may be identified as the Cauchy mean or hydrostatic stress

$$\sigma_{ij}^{\text{dil}} = p\delta_{ij}$$

- ▶ For computations we let  $\bar{J}$  be related to  $\theta$  through

$$\bar{J} = 1 + \theta \Rightarrow \theta = 0 \quad \text{in} \quad C_0$$

## Linearized discrete form of the variational equations

- ▶ If we approximate the volume change  $\theta$  and the pressure  $p$  by interpolation functions in reference coordinates  $\mathbf{X}$

$$\theta = \sum_{b=1}^{n_\theta} L_b(\mathbf{X}) \tilde{\theta}_b = \mathbf{L} \tilde{\boldsymbol{\theta}} \quad \text{and} \quad p = \sum_{b=1}^{n_p} M_b(\mathbf{X}) \tilde{p}_b = \mathbf{M} \tilde{\mathbf{p}}$$

the linearized discrete form of the variational equation reads

$$\begin{bmatrix} \mathbf{K}_{uu} & \mathbf{K}_{u\theta} & \mathbf{K}_{up} \\ \mathbf{K}_{\theta u} & \mathbf{K}_{\theta\theta} & \mathbf{K}_{\theta p} \\ \mathbf{K}_{pu} & \mathbf{K}_{p\theta} & \mathbf{0} \end{bmatrix} \begin{Bmatrix} d\tilde{\mathbf{u}} \\ d\tilde{\boldsymbol{\theta}} \\ d\tilde{\mathbf{p}} \end{Bmatrix} = \begin{Bmatrix} \mathbf{R}_u \\ \mathbf{R}_\theta \\ \mathbf{R}_p \end{Bmatrix}$$

- ▶ Residuals are expressed as sums over elements as

$$\begin{aligned} \mathbf{R}_u &= \mathbf{f} - \sum_e \int_{\Omega_e} \mathbf{B}^T \hat{\boldsymbol{\sigma}} \bar{J} d\Omega & \hat{\boldsymbol{\sigma}} &= \bar{\boldsymbol{\sigma}} + \mathbf{m}(\hat{p} - \bar{p}) \\ \mathbf{R}_\theta &= \sum_e \int_{\Omega_e} \mathbf{L}^T (\bar{p} - p) d\Omega & \bar{p} &= \frac{1}{3} \mathbf{m}^T \bar{\boldsymbol{\sigma}} \\ \mathbf{R}_p &= \sum_e \int_{\Omega_e} \mathbf{M}^T (J - \bar{J}) d\Omega & \hat{p} &= (J/\bar{J}) p \\ & & \mathbf{m}^T &= [1, 1, 1, 0, 0, 0] \end{aligned}$$

## Discontinuous $\theta - p$ approximations

- ▶ Approximations for  $\theta$  and  $p$  are identical ( $\mathbf{L} = \mathbf{M}$ ) and assumed to be discontinuous between contiguous elements

$\Rightarrow \tilde{\boldsymbol{\theta}}$  and  $\tilde{\mathbf{p}}$  are condensed out on the element level

- ▶ Direct solution  $\Rightarrow \mathbf{R}_\theta^e$  and  $\mathbf{R}_p^e$  vanish and the linearized form is reduced to

$$\bar{\mathbf{K}}_{uu} d\tilde{\mathbf{u}} = \mathbf{R}_u$$

where

$$\bar{\mathbf{K}}_{uu} = \mathbf{K}_{uu} + \mathbf{K}_{up} \mathbf{K}_{\theta p}^{-1} \mathbf{K}_{\theta\theta} \mathbf{K}_{p\theta}^{-1} \mathbf{K}_{pu} - \mathbf{K}_{u\theta} \mathbf{K}_{\theta p}^{-1} \mathbf{K}_{pu} - \mathbf{K}_{up} \mathbf{K}_{\theta p}^{-1} \mathbf{K}_{\theta u}$$

- ▶ An efficient procedure to compute the reduced tangent may be found in<sup>3</sup>

---

<sup>3</sup>Zienkiewics, O.C. and Taylor, R.L. The Finite Element Method for Solid and Structural Mechanics (6th ed, Elsevier, 2005)

## $Q_p/P_{p-1}$ and $Q_p/Q_{p-1}$ mixed formulations

- ▶ Implemented and studied two different constraint approximations based on the three-field variational form:

$Q_p/P_{p-1}$ :  $\mathbf{u}$  continuous of order  $p$  with  $C^{p-1}$  continuity on "patches",  $\theta$  and  $p$  discontinuous of order  $p - 1$

**Note:**  $\theta$  and  $p$  are expanded in individual Lagrange elements whereas for Splines  $\theta$  and  $p$  are expanded in individual knot-spans  $\Rightarrow$  as the polynomial order increases the pressure space for Splines increases compared to Lagrange

$Q_p/Q_{p-1}$ :  $\mathbf{u}$  continuous of order  $p$  with  $C^{p-1}$  continuity on "patches",  $\theta$  and  $p$  also continuous, but of order  $p - 1$  with  $C^{p-2}$  continuity on "patches"

## Babuška–Brezzi condition – Volumetric locking

- ▶ To avoid volumetric locking the Babuška–Brezzi condition must be satisfied

$$n_u \geq n_\theta = n_p$$

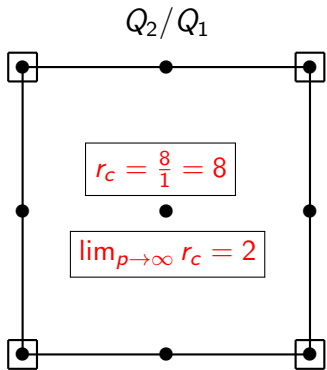
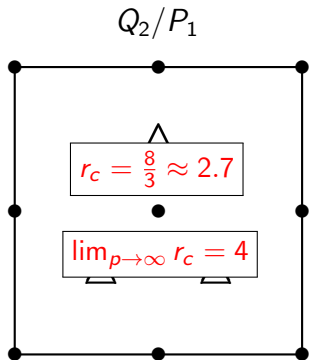
where  $n_u$ ,  $n_\theta$  and  $n_p$  denote the number of unknown displacement  $\tilde{\mathbf{u}}$ , volume  $\tilde{\theta}$ , and pressure parameters  $\tilde{\mathbf{p}}$

- ▶ In order to predict the propensity of volumetric locking, we define the constraint ratio

$$r_c = \frac{n_u}{n_p} = \frac{n_u}{n_\theta}$$

- ▶ The ideal value of the ratio  $r_c$  would then be the ratio between number of equilibrium equations ( $= n_{sd}$ ), divided by number of incompressibility conditions ( $=1$ )  
 $\Rightarrow r_c = n_{sd} \Rightarrow$  the ideal ratio would be  $r_c = 2$  in 2D
- ▶ If  $r_c < n_{sd}$  volumetric locking may be anticipated

## $Q_2/P_1$ and $Q_2/Q_1$ mixed Lagrange elements

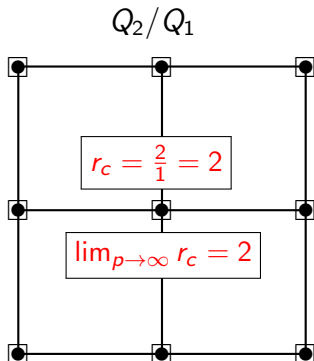
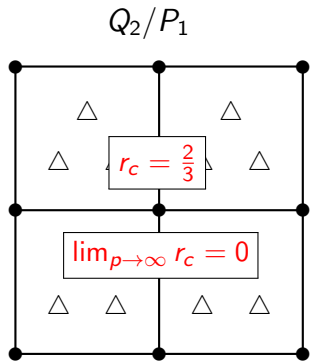


● = Displacement node

□ = Pressure/volume change node

△ = Internal pressure/volume change node

## $Q_2/P_1$ and $Q_2/Q_1$ mixed Spline elements



● = Displacement node

□ = Pressure/volume change node

△ = Internal pressure/volume change node

## Implementational issues

- ▶ *IFEM* : Object-oriented toolbox for isogeometric FE analysis
  - ▶ Problem-independent computational core
  - ▶ 2D and 3D continuum formulations, Kirchoff–Love thin plate and shell formulations
  - ▶ Lagrange, Spectral, Splines and NURBS basis functions
- ▶ Basis function evaluation (Splines/NURBS) based on GoTools  
<http://www.sintef.no/Projectweb/Geometry-Toolkits/GoTools>
- ▶ Element-level linear algebra: Use machine-optimized **BLAS**
  - ▶ For higher-order elements, the element matrices become large
  - ▶ Important to express the nonlinear FE formulation on *matrix* form (Voigt notation) — not *tensor* form
- ▶ Linear equation solvers
  - ▶ SuperLU (direct methods) <http://crd.lbl.gov/~xiaoye/SuperLU>
  - ▶ PETSc (iterative methods) <http://www.mcs.anl.gov/petsc>
  - ▶ Parallelization in progress (based on MPI message passing)

# Implementing the weak form (reference config.)

- ▶ Using tensor notation:

$$k_{mn}^{ab} = \int_{\Omega_0} N_{a,i} F_{mj} C_{ijkl} F_{nk} N_{b,l} d\Omega$$

- ▶ Gives 8 nested loops, within the integration point loop!!

```
for (a = 1; a <= N.size(); a++)
  for (b = 1; b <= N.size(); b++)
    for (m = 1; m <= nsd; m++)
      for (n = 1; n <= nsd; n++)
        {
          double km = 0.0;
          for (i = 1; i <= nsd; i++)
            for (j = 1; j <= nsd; j++)
              for (k = 1; k <= nsd; k++)
                for (l = 1; l <= nsd; l++)
                  km += dNdX(a,i)*F(m,j)*D(i,j,k,l)*F(n,k)*dNdX(b,l);

          EM(nsd*(a-1)+m,nsd*(b-1)+n) += km*detJW;
        }
}
```

- ▶ 11400 DOFs  $\Rightarrow$  48s CPU time for one element assembly step (89% of total simulation time)  
T = 2665s

- ▶ Using Voigt notation:

$$\mathbf{k} = \int_{\Omega_0} \mathbf{B}^T \mathbf{D}_T \mathbf{B} d\Omega$$

- ▶ Implemented by two calls to BLAS-subroutine DGEMM

- ▶ 11400 DOFs  $\Rightarrow$  19s CPU time for one element assembly step (82% of total simulation time)  
T = 1176s

# Numerical examples

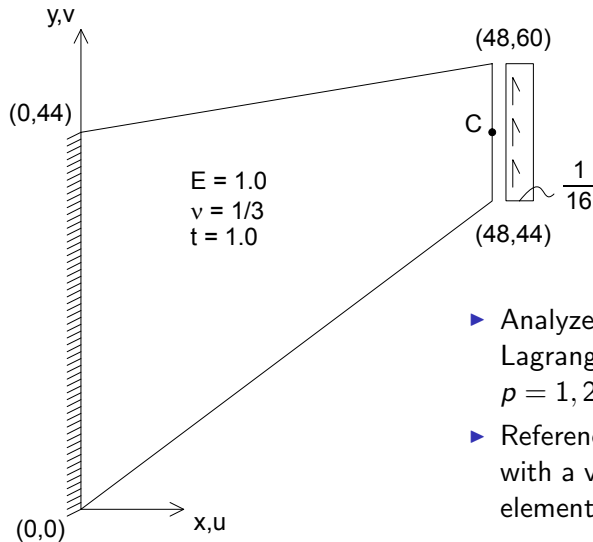
## Numerical examples

- ▶ The performance of the three-field mixed forms:
  - ▶  $Q_p/P_{p-1}$  : discontinuous  $p$  and  $\theta$ , and
  - ▶  $Q_p/Q_{p-1}$  : continuous  $p$  and  $\theta$

is numerically assessed and compared to the one-field  $Q_p$  displacement formulation with Splines and Lagrange basis functions

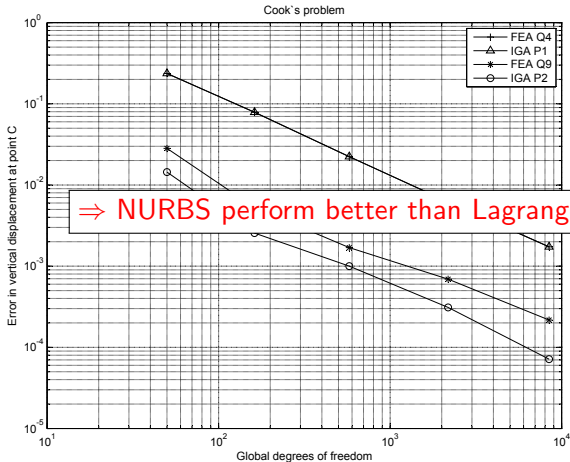
- ▶ The accuracy and the convergence characteristics are assessed in the finite deformation regime for elastic and elasto-plastic materials

## Cook's problem: Linear plane stress problem



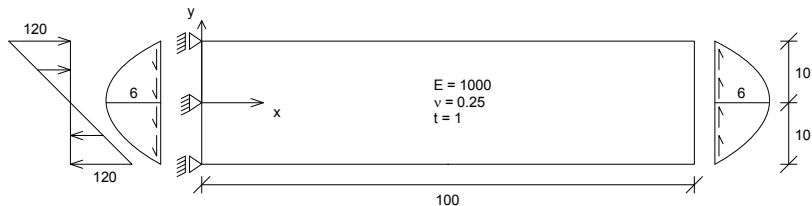
- ▶ Analyzed with NURBS and Lagrange  $Q_p$  elements,  $p = 1, 2$
- ▶ Reference solution obtained with a very fine mesh of LST elements (ndof = 41586)

# Cook's problem: Error in vertical tip displacement, $v_C$



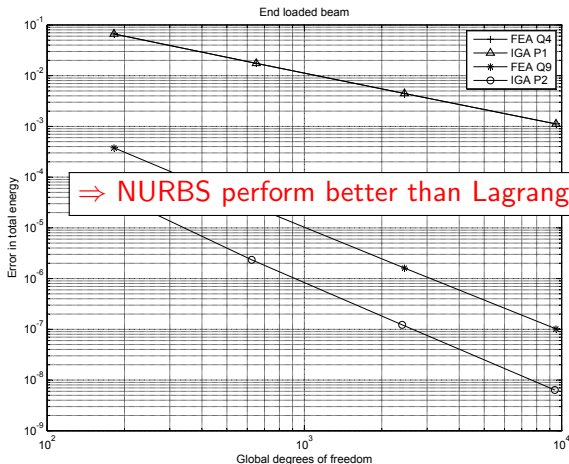
- ▶ As expected NURBS and Lagrange elements of polynomial order  $p = 1$  coincide
- ▶ NURBS converge at the same rate but is more accurate than Lagrange elements of polynomial order  $p = 2$

## End loaded cantilever beam: Linear plane stress problem



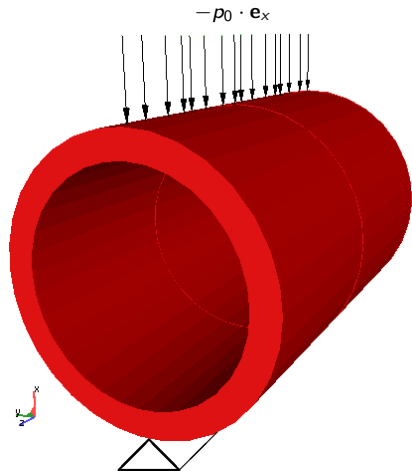
- ▶ Exact solution may be obtained for this particular problem
- ▶ Analyzed with NURBS and Lagrange  $Q_p$  elements,  $p = 1, 2$
- ▶ Note: In order to be compatible with the exact solution, a parabolic transverse traction field acting downward and a normal traction field equivalent to the transverse shear force and the moment, respectively, must be applied to the supported end

# End loaded cantilever beam: Error in potential energy



- ▶ As expected NURBS and Lagrange elements of polynomial order  $p = 1$  coincide
- ▶ NURBS converge at the same rate but is more accurate than Lagrange elements of polynomial order  $p = 2$

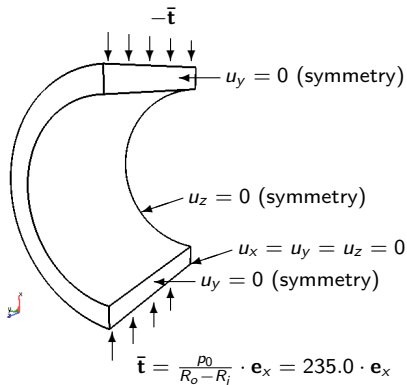
# Compression of a Thick Cylinder



Length	:	$L = 30.0$
Outer radius	:	$R_o = 10.0$
Inner radius	:	$R_i = 8.0$
Young's modulus	:	$E = 16800$
Poisson's ratio	:	$\nu = 0.4$
Load intensity	:	$\rho_0 = 470.0$

Note: Quadratic NURBS describe exact geometry in  $C_0$  !

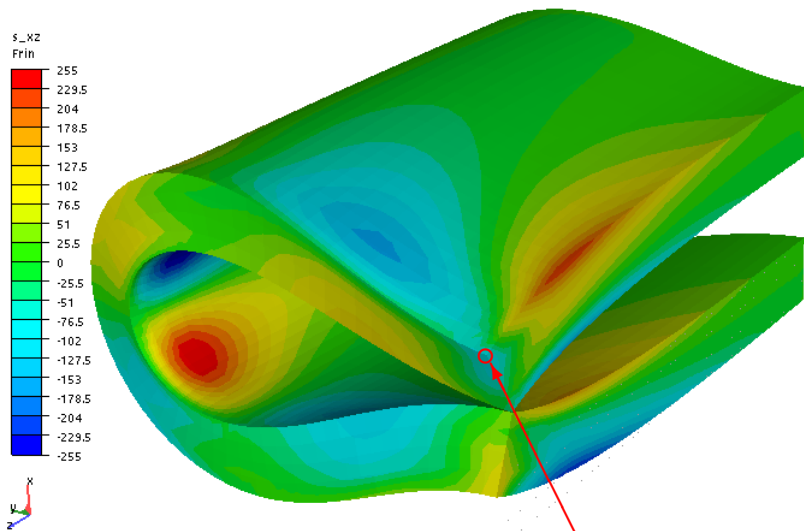
# Compression of a Thick Cylinder



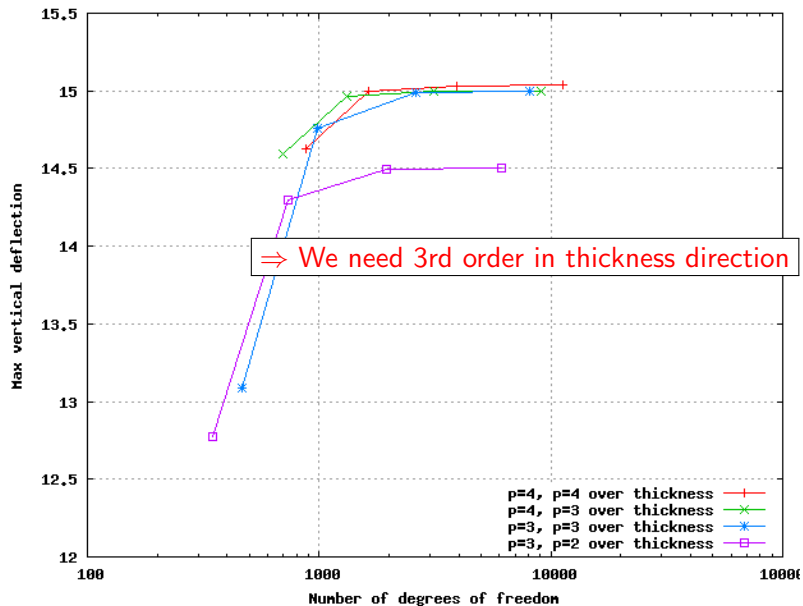
- ▶ Due to symmetry, only one quarter is modelled
  - ▶ One element over the thickness, varying in length and circumferential direction
  - ▶ NURBS and Lagrange  $Q_p$  elements,  $p = 2, 3, 4$
  - ▶ Compressible neo-Hookean material model
- $$\Psi(J, \mathbf{b}) = \frac{1}{2}\mu(\text{tr}\mathbf{b}-3) - \mu \ln J + \frac{1}{2}\lambda(\ln J)^2$$
- ▶ Load is here applied as two oppositely directed tangential tractions

# Compression of a Thick Cylinder

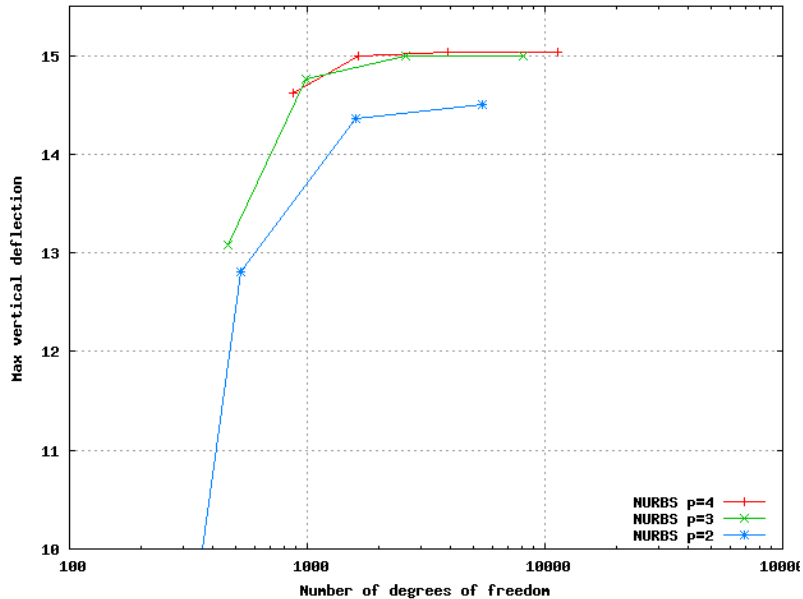
Deformed configuration with the Cauchy stress  $\sigma_{xz}$



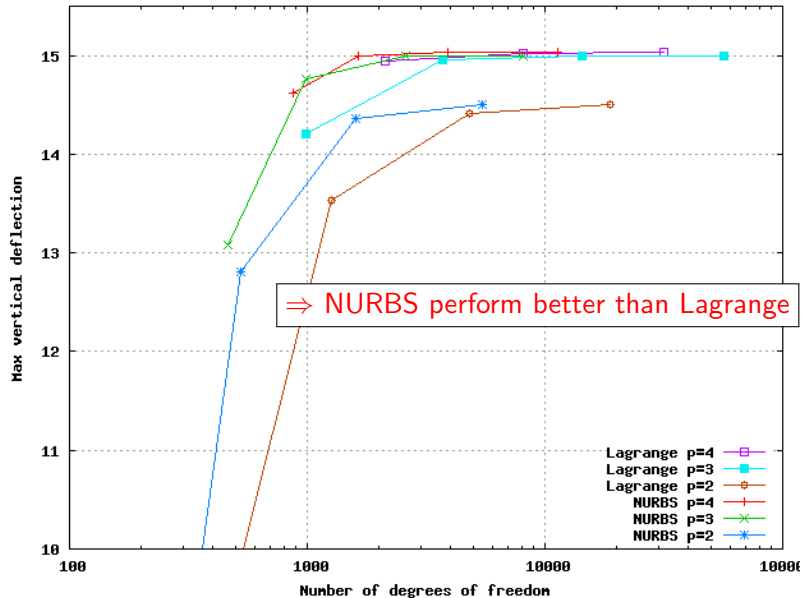
## Considering basis order through thickness (NURBS)



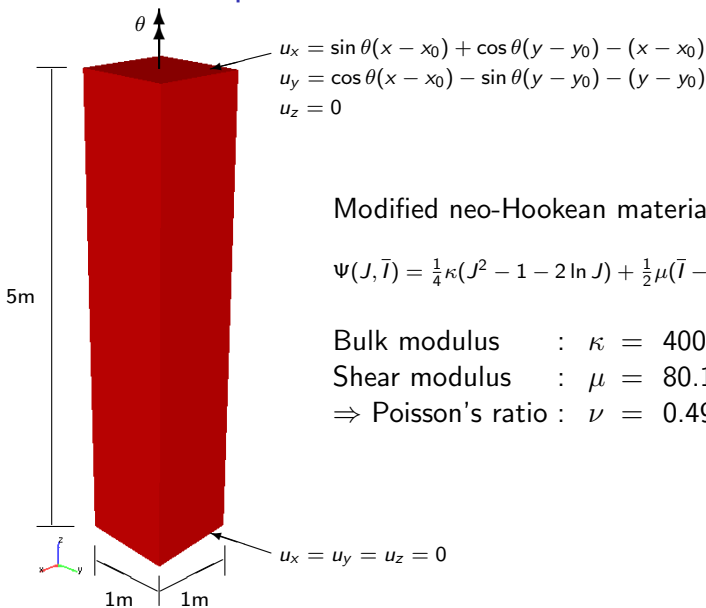
# Convergence for NURBS



# Convergence for NURBS and Lagrange



## Torsion of a square column

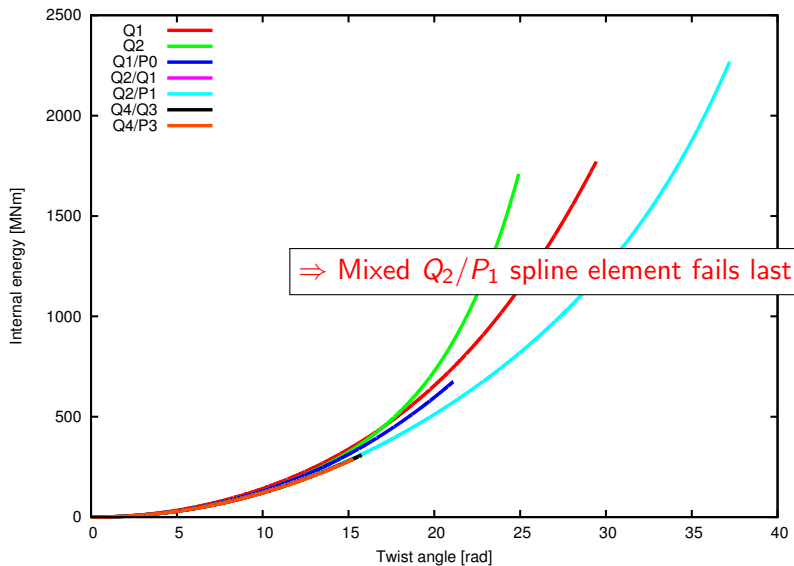


Torsion of a square column:  $Q_2/P_1$  ( $\theta = 10.0 \text{ rad} \approx 573^\circ$ )



- ▶  $5 \times 5 \times 17$  control points  
⇒ 1125 DOFs
- ▶ Analyzed with both  $Q_p$ ,  
 $Q_p/P_{p-1}$  and  $Q_p/Q_{p-1}$   
elements ( $p = 1, 2, 3, 4$ )
- ▶ Increment size:  $d\theta = 0.01$

## Stored elastic strain energy for spline elements



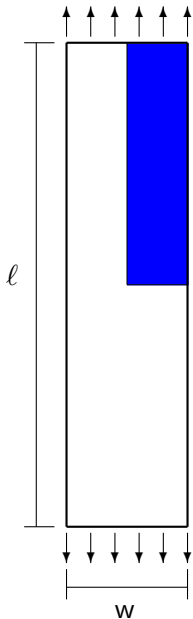
## Torsion of a square column: Failure angle ( $\theta_f$ )

Approx.	Grid	Formulation	$\theta_f$ [rad]
Lagrange/ Splines	$4 \times 4 \times 16$	Q1	29.45
		Q1/P0	21.12
Lagrange	$2 \times 2 \times 8$	Q2	10.39
		Q2/P1	19.22
Splines	$3 \times 3 \times 15$	Q2	24.93
		Q2/P1	37.22
Splines	$2 \times 2 \times 14$	Q3	23.86
		Q3/P2	27.36
Lagrange	$1 \times 1 \times 4$	Q4	0.12
		Q4/P3	14.96
Splines	$1 \times 1 \times 13$	Q4	0.27
		Q4/P3	15.30

Number of degrees of freedom = 1125 for all grids !

Prescribed incremental size  $d\theta = 0.01$  [rad] for all analyses !

# Necking of elastic-plastic tension strip:



► Geometry:

Length :  $\ell = 53.334$   
Width :  $w = 12.826$   
Center width :  $w_c = 0.982w$

► Finite strain elastic-plastic model with a  $J_2$  yield function; uniaxial yield stress given by:

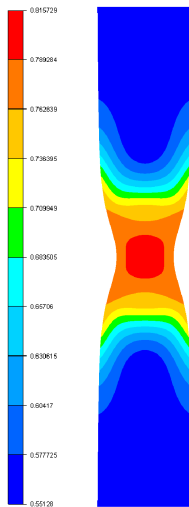
$$\sigma_y = \sigma_\infty + (\sigma_0 - \sigma_\infty) \exp(-\beta e_p) + \sqrt{\frac{2}{3}} h e_p$$

Bulk modulus :  $\kappa = 164.206$   
Shear modulus :  $\mu = 80.1938$   
Initial yield stress :  $\sigma_0 = 0.45$   
Residual yield stress :  $\sigma_\infty = 0.715$   
Isotropic hardening :  $h = 0.12924$   
Saturation exponent :  $\beta = 16.93$   
Effective plastic strain :  $e_p$

## Necking of elastic-plastic tension strip:



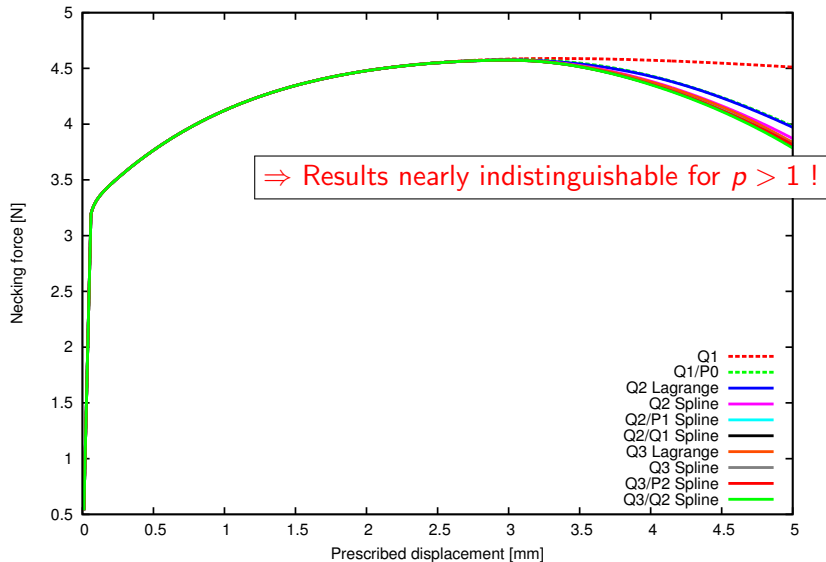
a) Mesh for one quadrant of the strip with 6 knot spans in the width and 12 in length  $\Rightarrow 7 \times 13$  grid points (basis functions)



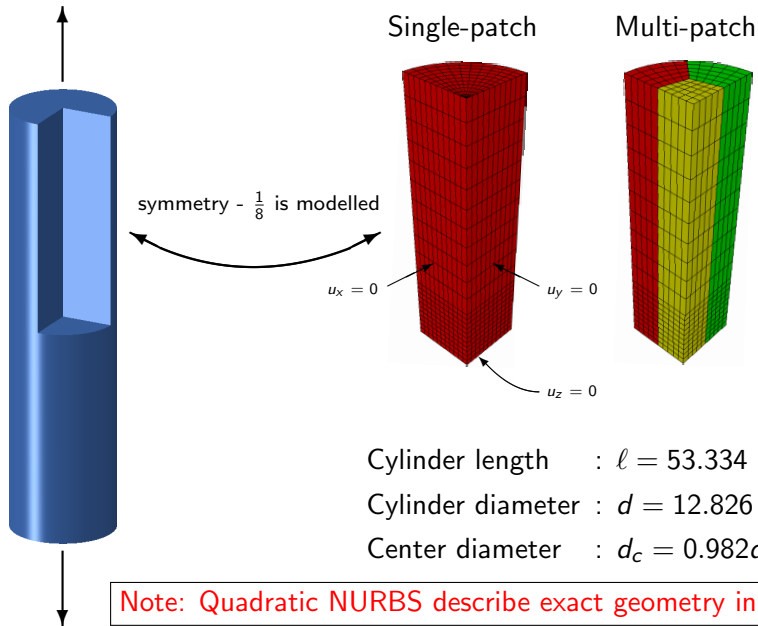
b) Mises stress distribution at final configuration obtained with the  $Q_3/P_2$  spline element with a  $49 \times 97$  grid



# Necking of elastic-plastic tension strip : $7 \times 13$ grid points

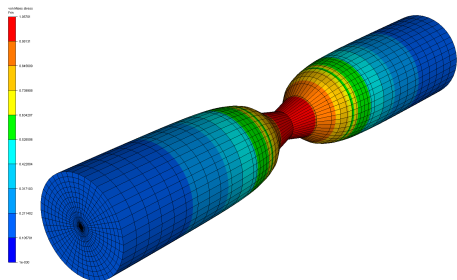


# Necking of elastic-plastic cylinder

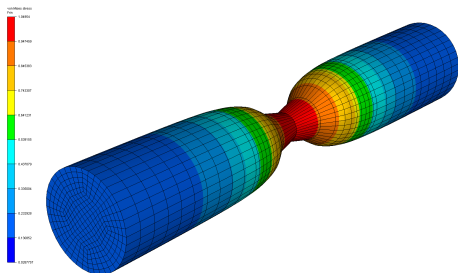


# Necking of elastic-plastic cylinder

Single-patch analysis

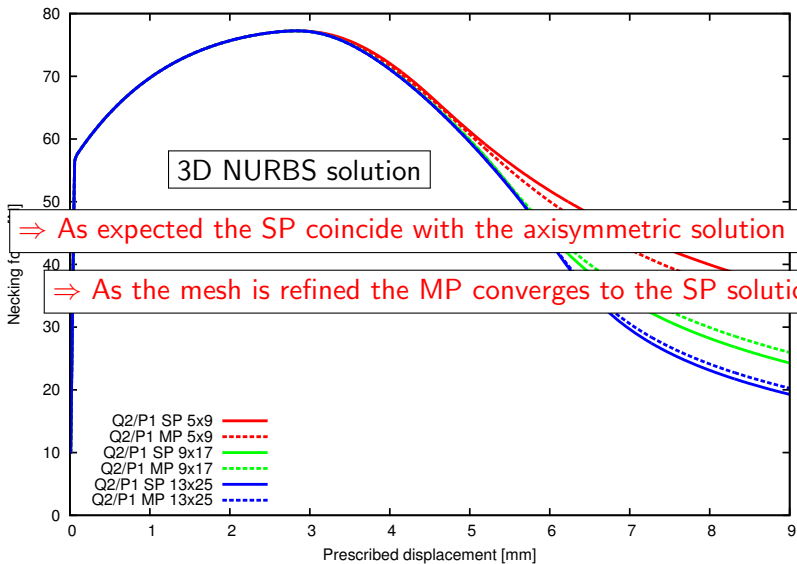


Multi-patch analysis



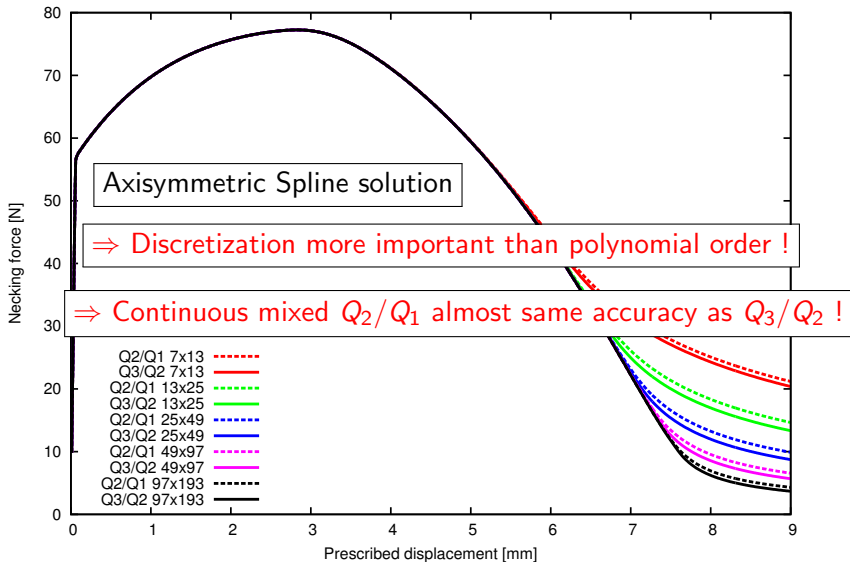
- ▶ Mises stress distribution at final configuration
- ▶ Three dimensional analysis
- ▶ Approximation:  $Q_2$  NURBS element
- ▶ Discretization:  $13 \times 25$  control points

# Necking of elastic-plastic cylinder : $Q_2/P_1$ NURBS element

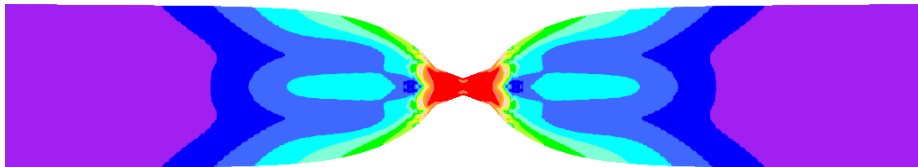




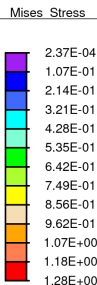
# Necking of elastic-plastic cylinder : $Q_p/Q_{p-1}; p = 2, 3$



# Necking of elastic-plastic cylinder



- ▶ Mises stress distribution at final configuration
- ▶ Axisymmetric analysis
- ▶ Approximation:  $Q_3/P_2$  mixed spline element
- ▶ Discretization:  $151 \times 301$  control points
- ▶ Number of unknowns: 90 299



Time = 9.00E+00

## Concluding remarks:

- ▶ By means of numerical examples, the performance of isogeometric Splines and NURBS elements have been assessed on problems involving *compressible* and *nearly incompressible* hyperelasticity and finite multiplicative plasticity
- ▶ A remarkable ability in capturing strain localization phenomena has been verified for both *plane strain*, *axisymmetric* and *three-dimensional* isogeometric solid elements
- ▶ While *continuous* mixed  $Q_p/Q_{p-1}$  is preferable for both nearly incompressible elastic materials and finite strain plasticity
- ▶ *Discontinuous* mixed  $Q_p/P_{p-1}$  is far more efficient in terms of computer resources
- ▶ Further work:
  - ▶ A more detailed study of the 3D necking problem with *adaptively refined* meshes in the necking zone
  - ▶ Isogeometric finite element analysis of *thin-walled* structures

*Thank you for your attention!*